

**Relation between spontaneous polarization and crystal field from first principles**

A. Belabbes, J. Furthmüller, and F. Bechstedt

*Institut für Festkörpertheorie und -optik, Friedrich-Schiller-Universität, Max-Wien-Platz 1, 07743 Jena, Germany*

(Received 14 June 2012; revised manuscript received 24 November 2012; published 10 January 2013)

Recently several hexagonal polytypes of III-V compounds have been discovered during growth of nanowires. They exhibit a spontaneous polarization. We calculate the polarization using the *ab initio* density functional theory within the Berry phase and the electrostatic method. We demonstrate its clear relationship to the crystal field characterized by internal-cell parameters and polytype hexagonality. Sign and magnitude of the polarization field in wurtzite follow the deviation of the internal-cell parameter from its ideal value, thereby explaining the opposite behavior of III-nitrides and the corresponding phosphides, arsenides, and antimonides.

DOI: [10.1103/PhysRevB.87.035305](https://doi.org/10.1103/PhysRevB.87.035305)

PACS number(s): 61.46.Km, 73.61.Ey, 77.70.+a, 78.67.Qa

**I. INTRODUCTION**

Spontaneous polarization occurs in ionic materials which underly a certain symmetry break.<sup>1,2</sup> For instance, ionic crystals with a singular polar axis exhibit such a spontaneous polarization field  $P_{sp}$ , i.e., they are pyroelectric. However, there are conceptual challenges: The spontaneous polarization of a crystal is actually not well defined; it depends on the chosen gauge.<sup>3,4</sup> Moreover, only polarization differences can be experimentally accessed.<sup>1,2</sup> They are visible as pyroelectricity at surfaces or interfaces or as consequences of internal electric fields in quantum well structures, for example, as quantum confined Stark effect.<sup>5</sup>

The strength of the spontaneous polarization field depends on the ionicity of the chemical bonds and the local symmetry break, for instance, the deformation of the bonding tetrahedra in fourfold coordinated compounds. These facts have been used to derive point-charge models for the spontaneous polarization.<sup>6,7</sup> However, a clear relationship between ionic bonds and the crystal field characterizing the symmetry break is still missing. This holds especially for the sign of  $P_{sp}$  in the case of weak ionicity and small deviations from cubic symmetry.

An important class of ionic materials that exhibits effects of the spontaneous polarization are semiconductors that crystallize in the wurtzite (wz, 2H) structure with space group  $P6_3mc$  ( $C_{6v}^4$ ). Among them, AlN, GaN, and InN stand out as materials for solid-state lighting.<sup>8</sup> Both the color and the luminous efficacy of nitride-based light sources critically depend on  $P_{sp}$ .<sup>5,9</sup> Therefore,  $P_{sp}$  has been intensively studied theoretically<sup>7,10,11</sup> and experimentally.<sup>5,12–14</sup> Large polarization fields up to  $P_{sp} = -0.04$  C/m<sup>2</sup> (AlN<sup>12</sup>) and  $-0.02$  C/m<sup>2</sup> (GaN<sup>13,14</sup>) have been observed.

The majority of other semiconducting III-V compounds does not show a spontaneous polarization since they crystallize in cubic zinc-blende (zb, 3C) geometry with space group  $F\bar{4}3m$  ( $T_d^2$ ) under ambient conditions. However, growth of conventional III-V compounds such as Ga- and In-derived phosphides, arsenides, and antimonides in form of [111]-oriented nanowires indicates a random intermixing of zb and wz stackings.<sup>15</sup> Controlling the crystallographic phase purity of III-V nanowires is notoriously difficult. However, recently enormous progress has been made in controlled growth of twin-plane or polytypic superlattices.<sup>16,17</sup> Even pure wurtzite nanowires have been grown.<sup>18</sup> One already speaks about

polytypism of III-V compounds.<sup>19</sup> Besides the well-known hexagonal crystal structure with wurtzite geometry, denoted by 2H, also other hexagonal polytypes, 4H and 6H, with the same space group have been observed.<sup>20–22</sup> The hexagonal polytypes  $pH$  ( $p = 2, 4, 6$ ) differ with respect to the bonding topology of cation-anion bilayers in [0001] direction as indicated in Fig. 1. Translational symmetry is reached after  $p$  bilayers, in contrast to the cubic zb or 3C polytype which is periodic in [111] direction after three bilayers.<sup>19</sup> One can distinguish cubic and hexagonal bilayers according to the stacking in the neighboring bilayers. Since in 2H (3C) only hexagonal (cubic) bilayers occur, one may count two hexagonal bilayers in 4H and 6H. This allows the definition of a polytype hexagonality  $h = 2/p$ .

All these hexagonal polytypes should exhibit spontaneous polarization  $P_{sp}$ , which will significantly influence the electronic and optoelectronic action of noncubic nanowires. This especially holds for heterocrystalline junctions and superlattices.<sup>16,17</sup> The presence of interfaces between two polytypes of one-and-the-same compound in [0001] direction significantly modifies the local electronic structure. The discovery of the hexagonal 2H, 4H, and 6H polytypes in nanorods of conventional III-V compounds asks for an understanding of the relationship between their atomic geometry and the resulting polarization field. How do the local bonding geometries influence the magnitude and the sign of  $P_{sp}$ ? Which structural parameters are the most important ones? Are the ionic bonds influenced by the actual stacking?

In this paper we study these questions for prototypical hexagonal III-V compounds in their bulk form from first principles. The methods used are briefly described in Sec. II. In the following section, Sec. III, results for the geometrical input and the polarization fields are presented and discussed. Finally, a brief summary is given in Sec. IV.

**II. METHODS AND APPROXIMATIONS**

Because of the fourfold coordination of cations and anions and the formation of bonding tetrahedra, the III-V compounds crystallizing in structures with hexagonal symmetry indeed represent model crystals for polarization studies. Any deformation of ideal tetrahedra, as such related to the hexagonal crystal field, gives rise to spontaneous polarization. The effect of the nanorod surfaces perpendicular to the stacking

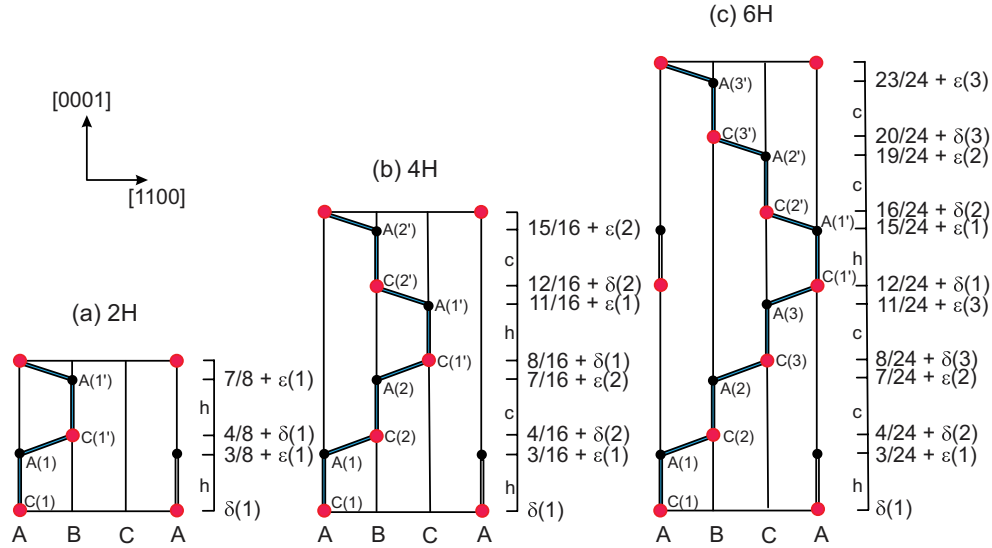


FIG. 1. (Color online) Bonding chains in  $(11\bar{2}0)$  planes of hexagonal polytypes. One unit cell, the stacking AB... as well as the cubic ( $c$ ) or hexagonal ( $h$ ) character of a cation (C)-anion (A) bilayer are indicated. The internal-cell parameters, the deviations from the ideal tetrahedral geometry,  $\delta(i)$  and  $\epsilon(i)$  ( $i = 1, \dots, p/2$ ), are indicated.

direction is omitted. According to the existence of one singular polar axis only the component  $P_{sp}$  parallel to this axis is studied. We apply two different conceptual and computational schemes for the spontaneous polarization, more precisely its component parallel to the hexagonal axis. First, we use the Berry-phase approach<sup>1,2</sup> of Ref. 23 as implemented in the Vienna *ab initio* simulation package (VASP).<sup>24</sup> Results are obtained in the framework of the density-functional theory (DFT) within the local density approximation (LDA) where the exchange-correlation (XC) functional is parametrized according to Perdew and Zunger.<sup>25</sup> The outermost  $s$ ,  $p$ , and (for Ga and In)  $d$  electrons are treated as valence electrons within the projector-augmented wave (PAW) method.<sup>26</sup> Outside the cores the electronic wave functions are expanded into plane waves up to an energy cutoff of 500 eV. The Brillouin zone (BZ) integrations are carried out on  $\Gamma$ -centered  $10 \times 10 \times M$   $\mathbf{k}$ -point meshes with  $M = 10, 6, 3, 2$  for the 3C, 2H, 4H, and 6H polytype, respectively. Second, for the purpose of comparison we also apply an electrostatic method<sup>3,7,27</sup> which allows the direct computation of the internal electric field in a hexagonal polytype restricted by interfaces to zb layers. More in detail, the macroscopic electrostatic potential is computed for  $(pH)_{12/p}(3C)_4$  superlattices from the Kohn-Sham potential of the DFT.

Both methods require an accurate determination of the atomic coordinates and, hence, of the crystal field. To compute the difference between the polarization in  $pH$  and zinc blende we optimize the atomic geometries of the four polytypes 3C, 2H, 4H, and 6H of 12 Al, Ga, and In compounds, more precisely nitrides, phosphides, arsenides, and antimonides. Each hexagonal polytype possesses a finite number of parameters, two lattice constants  $c$  and  $a$  and  $(p - 1)$  internal-cell parameters, which are indicated by shifts  $\delta(i)$  and  $\epsilon(i)$  ( $i = 1, \dots, p/2$ ) in units of lattice constant  $c$  in Fig. 1. With  $\delta(1) \equiv 0$  indeed the number  $(p - 1)$  is maintained. Together with the cell-shape parameter  $2c/(pa)$  they characterize the crystal field. In the simple case of wurtzite the single internal-cell

parameter is denoted by  $u$  with  $u = \frac{3}{8} + \epsilon(1)$ . It characterizes the length  $uc$  of the bonds parallel to the  $c$  axis. For ideal, nondeformed bonding tetrahedra it holds  $c/a = \sqrt{8/3}$  and  $u_{ideal} = 3/8$ . Deviations from these values characterize the hexagonal crystal field in 2H. For a given pair  $(c, a)$  of lattice constants the  $(p - 1)$  internal parameters are determined if the Hellmann-Feynman forces are smaller than 1 meV/Å. The lattice constants are fixed if the total energy of the polytype deviates less than 1 meV from its minimum.<sup>28,29</sup> All the calculations are performed within DFT-LDA. This method gives negative energy gaps and inverted band structures at  $\Gamma$  for InN, InAs, InSb, and GaSb, mainly due to an overestimation of the  $pd$  repulsion. Negative gaps however lead to drastic changes of the electrostatics of the polytypes and hence of the spontaneous polarization. In order to avoid the redistribution of electrons due to the wrong electronic structure, calculating the electrostatic potential we slightly open the gaps of the four compounds by applying the LDA-1/2 method<sup>29,30</sup> which can be interpreted as an approximate quasiparticle method.

### III. RESULTS AND DISCUSSION

#### A. Atomic geometry and crystal field

The hexagonal crystal field is characterized by internal-cell parameters, which are the atomic basis, and one cell-shape parameter, the ratio of the two lattice constants. Complete sets of internal-cell parameters are listed in Table I. The relative deviations of the atomic positions from their “ideal” ones only defined by the lattice constants  $c$  and  $a$  are small, in particular for conventional III-V compounds that crystallize in zinc-blende structure under ambient conditions. By contrast, the relative changes of group-III nitrides which crystallize in wurtzite structure under ambient conditions are much bigger and have an opposite sign in many cases, for example,  $\epsilon(1)$  (2H),  $\epsilon(2)$ ,  $\delta(2)$  (4H), and  $\epsilon(3)$ ,  $\delta(2)$  (6H).

TABLE I. Internal-cell parameters  $\varepsilon(i)$  and  $\delta(i)$  ( $i = 1, \dots, p/2$ ) for  $p$ H polytypes in units of  $10^{-4}$ .  $\delta(1) = 0$  has been chosen. The relative changes of the atomic coordinates are explained in Fig. 1.

Compound	2H		4H		6H				
	$\varepsilon(1)$	$\varepsilon(1)$	$\varepsilon(2)$	$\delta(2)$	$\varepsilon(1)$	$\varepsilon(2)$	$\varepsilon(3)$	$\delta(2)$	$\delta(3)$
AlN	40.0	27.0	27.0	-7.0	18.0	18.1	18.0	-4.6	-4.6
AlP	-1.0	2.5	-3.7	0.6	0.5	1.0	0.5	0.6	0.4
AlAs	-3.0	1.9	-3.9	1.7	0.5	1.0	0.6	0.5	0.5
AlSb	-1.0	1.9	-3.9	3.0	-1.6	-1.6	-1.6	1.7	1.7
GaN	10.0	6.4	6.4	-1.4	4.2	4.3	4.3	-0.8	-0.9
GaP	-4.0	2.2	-4.7	3.6	2.7	0.0	-3.8	3.5	-0.8
GaAs	-4.0	4.4	-3.5	5.3	2.8	0.0	-4.4	3.8	-0.5
GaSb	-7.0	0.1	-5.8	5.9	1.6	-1.3	-5.1	5.3	5.3
InN	20.0	14.1	14.1	-4.1	9.4	9.5	9.5	-2.7	-2.7
InP	-4.0	2.3	-3.1	1.8	1.4	-0.6	-1.5	0.9	0.6
InAs	-5.0	2.3	-3.7	3.0	1.8	-0.5	-2.3	1.6	0.1
InSb	-6.0	2.9	-3.2	4.7	1.9	-0.4	-2.6	2.5	0.0

Despite their smallness the optimization of the internal-cell parameters is important for finding the total-energy minimum with respect to  $c$  and  $a$  (see, e.g., Ref. 28).

The normalized cell-shape parameters  $2c/(pa)$  are listed for all hexagonal polytypes in Table II. In the wurtzite (2H) case the length  $u$  of the parallel bonds measured in units of the lattice constant  $c$  are also given in Table II. These parameters characterize the atomic geometries and finally also the crystal field by the deviations  $[2c/(pa) - 1.6333]$  (see Fig. 2) and  $(u - 0.375)$ . The computed  $2c/(pa)$  ratios are in excellent agreement with collections of available experimental data.<sup>10,20,31</sup> In Fig. 2 the lattice constant ratio  $2c/(pa)$  is plotted versus the percentage of hexagonality  $h$  of the polytype. It represents the ratio between hexagonal ( $h$ ) to the total [hexagonal and cubic ( $c$ )] bond stackings in a polytype, that is,  $h = 0$  (3C), 33 (6H), 50 (4H), and 100 (2H)%, as can be derived from Fig. 1. The topological trend is unique. It almost varies linearly with the hexagonality. The chemical trends are less obvious. Omitting the nitrides for a moment, for a given cation clear chemical trends are visible along the anion row P, As, and Sb. However, the ratios of the Al compounds are embedded between those of the Ga and In

ones due to missing semicore  $d$  electrons in Al. In addition (see inset of Fig. 2), there is a significant discrepancy between III-nitrides (which crystallize in wurtzite) and other III-V compounds (which crystallize in zinc blende). The  $2c/(pa)$  ratios for the wz-stable nitrides are smaller than the ideal value  $2c/(pa) = \sqrt{8/3}$ , while the zb-stable phosphides, arsenides, and antimonides have  $2c/(pa) > \sqrt{8/3}$ . These findings are in complete agreement with the predictions of Yeh *et al.*<sup>32</sup> for the zb-wz polytypism in semiconductors. Interestingly, the internal-cell parameter  $u$  of wz (see Table II) shows a similar behavior. For the nitrides, it holds  $u > 3/8$  (in agreement with other computations<sup>32</sup>), while all other III-V compounds show  $u < 3/8$ . The results can be explained by a balance of repulsive and attractive electrostatic interactions of bonds depending on their stacking, length, and ionic degree.<sup>33</sup> Interestingly, for the wurtzite polytype the relation  $u = \sqrt{3/8}a/c$  for ideal crystals is nearly fulfilled. In the average it holds  $\sqrt{8/3}c/au = 1.005$  for the 2H polytype of conventional III-V compounds, while  $\sqrt{8/3}c/au = 0.996$  is valid for nitrides. From this relation between cell shape and internal atomic positions one may conclude that, in principle, the crystal field can be characterized by one structural parameter, for example,  $2c/(pa)$ , in the average

TABLE II. Parameters of polytypes of III-V compounds being characteristic for the crystal field, the electronic screening, and the spontaneous polarization in Berry-phase (electrostatic) approach.

Compound	3C		6H		4H		2H	
	$\varepsilon_\infty$	$c/3a$	$P_{sp}(10^{-3} \text{ C/m}^2)$	$c/2a$	$P_{sp}(10^{-3} \text{ C/m}^2)$	$c/a$	$u$	$P_{sp}(10^{-3} \text{ C/m}^2)$
AlN	4.54	1.6223	-13 (-11)	1.6169	-20 (-17)	1.6014	0.3799	-40 (-34)
AlP	8.33	1.6369	2 (2)	1.6388	3 (3)	1.6449	0.3749	7 (6)
AlAs	9.40	1.6361	2 (2)	1.6377	3 (2)	1.6427	0.3747	6 (5)
AlSb	11.68	1.6358	0 (0)	1.6373	0 (0)	1.6418	0.3749	0 (0)
GaN	5.83	1.6316	-6 (-5)	1.6310	-9 (-7)	1.6293	0.3756	-18 (-15)
GaP	10.63	1.6370	1 (1)	1.6390	2 (2)	1.6443	0.3746	3 (3)
GaAs	14.59	1.6374	1 (2)	1.6396	1 (2)	1.6456	0.3746	2 (3)
GaSb	17.43	1.6376	1 (1)	1.6400	1 (2)	1.6459	0.3743	2 (3)
InN	12.44	1.6270	-1 (-4)	1.6244	-3 (-4)	1.6163	0.3775	-11 (-6)
InP	12.00	1.6356	0 (0)	1.6369	0 (0)	1.6408	0.3746	-1 (-1)
InAs	17.86	1.6360	0 (0)	1.6375	0 (0)	1.6419	0.3745	1 (1)
InSb	19.25	1.6330	0 (0)	1.6377	0 (0)	1.6424	0.3744	1 (1)

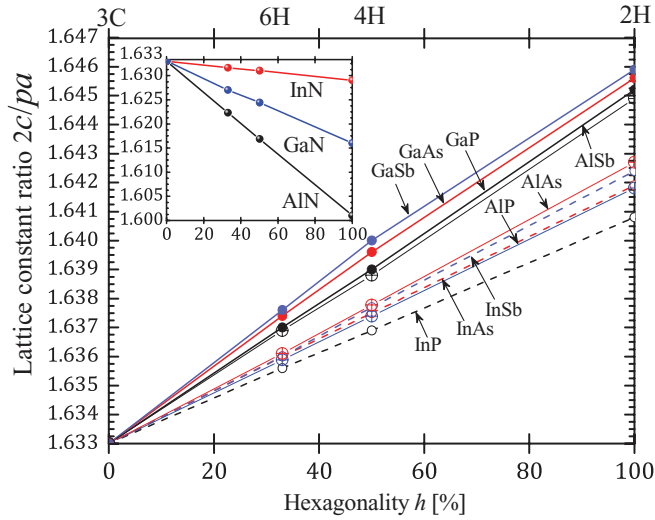
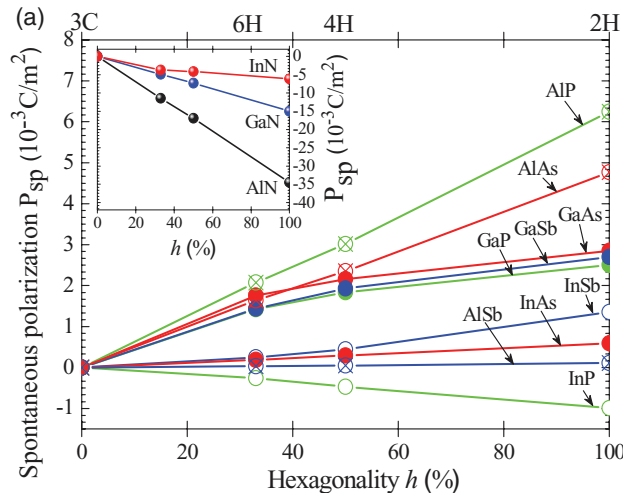


FIG. 2. (Color online) Ratio of the lattice constants  $2c/(pa)$  versus the polytype hexagonality.

instead of describing three (five) internal-cell parameters of 4H (6H), this parameter is listed in Table II.

### B. Spontaneous polarization

The polarization field values  $P_{sp}$  computed by means of the Berry phase as well as the electrostatic method are also listed in Table II. For completeness the static electronic dielectric constants  $\epsilon_{\infty}$  of the zinc-blende polytype are also given since they are needed within the electrostatic method.<sup>7,27</sup> The  $\epsilon_{\infty}$  values have been computed within the independent-particle approach. The structural trends are represented in Fig. 3, where the derived  $P_{sp}$  values are plotted versus the percentage of hexagonality. Since the hexagonality  $h$  is a certain global measure of the hexagonal crystal field, this figure illustrates the relation between polarization and crystal field. One can conclude that the absolute value of  $P_{sp}$  nearly linearly increases with  $h$ . Interestingly, this trend, the order of magnitude of  $P_{sp}$ , and the sign of  $P_{sp}$  do not depend on the method of calculation.



The method only influences somewhat the trends along the anion row Sb, As, P for the Ga and In cations with semicore  $d$  electrons. This is obvious from the comparison of Figs. 3(a) and 3(b). The chemical trend along the cations Al, Ga, and In is also independent of the computational method. The absolute values decrease along this row in average.

Most important is the dependence of the absolute values and the signs of the polarization on the crystal field. For phosphides, arsenides, and antimonides the spontaneous polarization field is positive while  $P_{sp} < 0$  holds for the nitrides. The only exception InP with  $P_{sp}(2H) \approx -1 \times 10^{-3} \text{ C/m}^2$  is related to a small absolute value. The values in Table II calculated for nitrides are close to results of recent measurements for wz-AlN<sup>12</sup> and wz-GaN.<sup>13,14</sup> Our absolute values 14–18 (GaN) and 33–40 (AlN)  $\times 10^{-3} \text{ C/m}^2$  are close to 21–22 (GaN) and 40 (AlN)  $\times 10^{-3} \text{ C/m}^2$  measured. Despite the use of the same methods different results have been obtained compared with previous calculations.<sup>7,10</sup> In the case of the electrostatic method the reason is obvious. Much too large values ( $u = 0.375$ ) have been used by Bechstedt *et al.*<sup>7</sup> resulting in too large absolute values of  $P_{sp}$ . The smaller overestimation in another computation<sup>10</sup> is a consequence of the use of pseudowave functions instead of all-electron PAW functions as here.

The relation of the sign of the structural quantities  $[2c/(pa) - \sqrt{8/3}]$  and  $(3/8 - u)$  with that of the spontaneous polarization  $P_{sp}$  in Table II and Fig. 3 together with the hexagonality trend of  $P_{sp}$  indicate a clear relationship between the “strength” of the hexagonal crystal field and the spontaneous polarization field.

In order to illustrate this relation in more detail we apply a point-charge model for the 2H polytype<sup>7</sup> (see derivation in Supplemental Material<sup>34</sup>)

$$P_{sp}^{\text{mod}} = -\frac{2ec}{\Omega_0} \left[ 4g_{\perp} \left( \frac{3}{8} - u \right) + (g_{\perp} - g_{\parallel})u \right], \quad (1)$$

with the unit-cell volume  $\Omega_0$ , and different charge-asymmetry coefficients  $g_{\perp}$  and  $g_{\parallel}$  according to bonds in a certain angle ( $g_{\perp}$ ) or bonds parallel ( $g_{\parallel}$ ) to the  $c$  axis. They slightly differ with respect to  $g$  of zinc blende.<sup>35</sup> Their difference may be

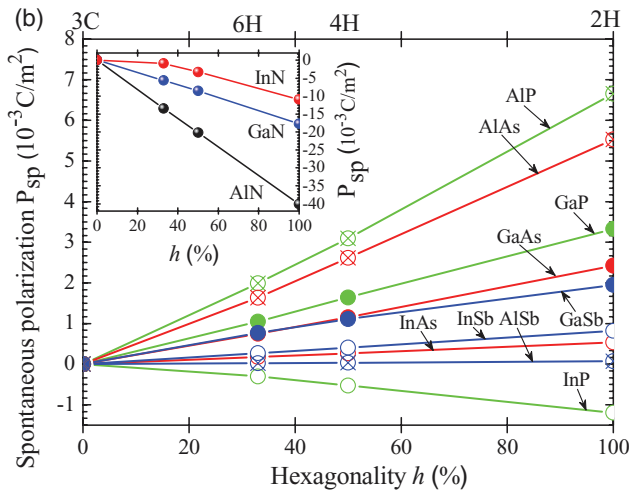


FIG. 3. (Color online) Strength  $P_{sp}$  of spontaneous polarization field versus polytype hexagonality for 12 III-V compounds as computed within the (a) electrostatic method and the (b) Berry-phase approach.



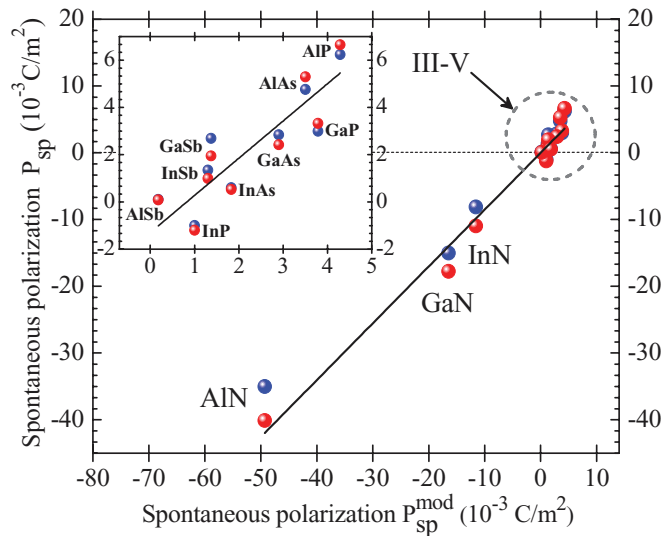


FIG. 4. (Color online) Computed polarization values  $P_{sp}$  versus polarization values estimated according to the bond charge model (1) for the 2H polytype. Bright red circles: Electrostatic model, dark blue circles: Berry-phase approach.

related to<sup>7</sup>

$$g_{\perp} - g_{\parallel} \approx \frac{1}{2}g(1 - g^2) \left[ \left( \frac{3}{8u} \right)^2 - \left( \frac{9}{8} \right)^2 \frac{1}{3a^2/c^2 + u^2} \right]. \quad (2)$$

Together with  $g_{\perp} \approx g$  in (1)  $P_{sp}^{\text{mod}}$  can be estimated.

In Fig. 4, for the 2H polytype, the  $P_{sp}$  values computed within the Berry phase and the electrostatic method are plotted versus the polarization  $P_{sp}$  within the point-charge model according to (1). In the average one observes a linear relationship. It is mainly governed by the first term in (1). The second one is much smaller because of the approximate relation  $u \approx \sqrt{\frac{3}{8} \frac{a}{c}}$ . In other words the parameter  $(u - 3/8)$  which has

been discussed to be most important for the characterization of the crystal field in wurtzite crystals also explains the absolute magnitude and the sign of the spontaneous polarization field in a hexagonal crystal with partial ionic bonding. The minor overestimation of the field strength in the point-charge model is probably a consequence of the overestimation of the ionic charges by the charge-asymmetry coefficients.<sup>35</sup> In any case, there is a clear relation between spontaneous polarization and crystal field.

#### IV. SUMMARY

In summary, the spontaneous polarization in hexagonal polytypes of III-V compound semiconductors has been studied within the Berry-phase method and an electrostatic superlattice approach based on the *ab initio* density functional theory. The latter framework has been also used to compute the cell shape and internal-cell geometry parameters which represent measures of the hexagonal crystal fields, and, hence, local deviations from the ideal bonding topology. These geometry parameters sensitively determine the spontaneous polarization  $P_{sp}$ . As a consequence, the absolute  $P_{sp}$  values linearly vary with the polytype hexagonality. The different magnitudes and signs of the polarization for III-nitrides and conventional III-V compounds (phosphides, arsenides, and antimonides) can be also explained by the crystal field. For the wurtzite polytype this has been clearly demonstrated by the proportionality to  $(u - u_{\text{ideal}})$ , that is the length variation of the bonds parallel to the hexagonal axis. We have to mention that biaxial strain fields which might be present in real quantum wires may lead to additional piezoelectric fields. They can be treated in a similar way if the strain state is known.

#### ACKNOWLEDGMENT

We acknowledge financial support from the Fonds zur Förderung der Wissenschaftlichen Forschung (Austria) in the framework of SFB 25 “Infrared Optical Nanostructures.”

<sup>1</sup>R. Resta, *Rev. Mod. Phys.* **66**, 899 (1994).

<sup>2</sup>R. Resta, *J. Phys.: Condens. Matter* **22**, 123201 (2010).

<sup>3</sup>M. Posternak, A. Baldereschi, A. Catellani, and R. Resta, *Phys. Rev. Lett.* **64**, 1777 (1990).

<sup>4</sup>A. K. Tagantsev, *Phys. Rev. Lett.* **69**, 389 (1992).

<sup>5</sup>O. Ambacher, J. Majewski, C. Miskys, A. Link, M. Hermann, M. Eickhoff, M. Stutzmann, F. Bernardini, V. Fiorentini, V. Tilak, B. Schaff, and L. F. Eastman, *J. Phys.: Condens. Matter* **14**, 3399 (2002).

<sup>6</sup>J. Jerphagnon and H. W. Newkirk, *Appl. Phys. Lett.* **18**, 245 (1971).

<sup>7</sup>F. Bechstedt, U. Grossner, and J. Furthmüller, *Phys. Rev. B* **62**, 8003 (2000).

<sup>8</sup>O. Brandt and K. H. Ploog, *Nat. Mater.* **5**, 769 (2006).

<sup>9</sup>P. Waltereit, O. Brandt, A. Trampert, H. T. Grahn, J. Menniger, M. Ramsteiner, M. Reiche, and K. H. Ploog, *Nature (London)* **406**, 865 (2000).

<sup>10</sup>F. Bernardini, V. Fiorentini, and D. Vanderbilt, *Phys. Rev. B* **56**, R10024 (1997).

<sup>11</sup>F. Bernardini, V. Fiorentini, and D. Vanderbilt, *Phys. Rev. B* **63**, 193201 (2001).

<sup>12</sup>S.-H. Park and S.-L. Chuang, *Appl. Phys. Lett.* **76**, 1981 (2000).

<sup>13</sup>G. Jacopin, L. Rigutti, L. Largeau, F. Fortuna, F. Furtmayr, F. H. Julien, M. Eickhoff, and M. Tchernycheva, *J. Appl. Phys.* **110**, 064313 (2011).

<sup>14</sup>J. Lähnemann, O. Brandt, U. Jahn, C. Pfüller, C. Roder, P. Dogan, F. Grosse, A. Belabbes, F. Bechstedt, A. Trampert, and L. Geelhaar, *Phys. Rev. B* **86**, 081302 (2012).

<sup>15</sup>H. J. Joyce, J. Wong-Leung, Q. Gao, H. H. Tan, and C. Jagadish, *Nano Lett.* **10**, 908 (2010).

<sup>16</sup>R. E. Algra, M. A. Verheijen, M. T. Borgstrom, L.-F. Feiner, G. Immink, W. J. P. van Enckevort, E. Vlieg, and E. P. A. M. Bakkers, *Nature (London)* **456**, 369 (2008).

- <sup>17</sup>P. Caroff, K. Dick, J. Johansson, M. Messing, K. Deppert, and L. Samuelson, *Nat. Nano* **4**, 50 (2009).
- <sup>18</sup>H. Shtrikman, R. Popovitz-Biro, A. Kretinin, L. Houben, M. Heiblum, M. Bukala, M. Galicka, R. Buczko, and P. Kacman, *Nano Lett.* **9**, 1506 (2009).
- <sup>19</sup>P. Käckell, B. Wenzien, and F. Bechstedt, *Phys. Rev. B* **50**, 10761 (1994).
- <sup>20</sup>D. Kriegner, C. Panse, B. Mandl, K. A. Dick, M. Keplinger, J. M. Persson, P. Caroff, D. Ercolani, L. Sorba, F. Bechstedt, J. Stangl, and G. Bauer, *Nano Lett.* **11**, 1483 (2011).
- <sup>21</sup>D. L. Dheeraj, G. Patriarche, H. Zhou, T. B. Hoang, A. F. Moses, S. Gronsborg, A. T. J. van Helvoort, B.-O. Fimland, and H. Weman, *Nano Lett.* **8**, 4459 (2008).
- <sup>22</sup>S. O. Mariager, C. B. Sørensen, M. Aagesen, J. Nygård, R. Feidenhans'l, and P. R. Willmott, *Appl. Phys. Lett.* **91**, 083106 (2007).
- <sup>23</sup>R. D. King-Smith and D. Vanderbilt, *Phys. Rev. B* **47**, 1651 (1993).
- <sup>24</sup>G. Kresse and J. Furthmüller, *Phys. Rev. B* **54**, 11169 (1996).
- <sup>25</sup>J. P. Perdew and A. Zunger, *Phys. Rev. B* **23**, 5048 (1981).
- <sup>26</sup>G. Kresse and D. Joubert, *Phys. Rev. B* **59**, 1758 (1999).
- <sup>27</sup>A. Qteish, V. Heine, and R. J. Needs, *Phys. Rev. B* **45**, 6534 (1992).
- <sup>28</sup>C. Panse, D. Kriegner, and F. Bechstedt, *Phys. Rev. B* **84**, 075217 (2011).
- <sup>29</sup>A. Belabbes, C. Panse, J. Furthmüller, and F. Bechstedt, *Phys. Rev. B* **86**, 075208 (2012).
- <sup>30</sup>L. G. Ferreira, M. Marques, and L. K. Teles, *Phys. Rev. B* **78**, 125116 (2008).
- <sup>31</sup>D. Kriegner, E. Wintersberger, K. Kawaguchi, J. Wallentin, M. T. Borgström, and J. Stangl, *Nanotechnology* **22**, 425704 (2011).
- <sup>32</sup>C.-Y. Yeh, Z. W. Lu, S. Froyen, and A. Zunger, *Phys. Rev. B* **46**, 10086 (1992).
- <sup>33</sup>T. Ito, T. Akiyama, and K. Nakamura, *Jpn. J. Appl. Phys.* **46**, 345 (2007).
- <sup>34</sup>See Supplemental Material at <http://link.aps.org/supplemental/10.1103/PhysRevB.87.035305> for relation between spontaneous polarization and crystal field.
- <sup>35</sup>A. García and M. L. Cohen, *Phys. Rev. B* **47**, 4215 (1993).